

Figure S1A: PDE4B expression in B cell lymphoma cell lines. Quantitative real-time RT-PCR based measurements define two groups of DLBCL cell lines with significantly distinct levels of PDE4B expression. The assays were performed in triplicate and the PDE4B expression was corrected by the expression of the actin gene. Data are displayed as relative expression determined using the $\Delta\Delta CT$ method, reported as $2^{-\Delta\Delta CT}$, and normalized by PDE4B expression in the DHL6 cell line (arbitrarily set at 1). DLBCL cell lines with PDE4B expression above or below the median (n=6) were classified as PDE4B-high and -low, respectively.

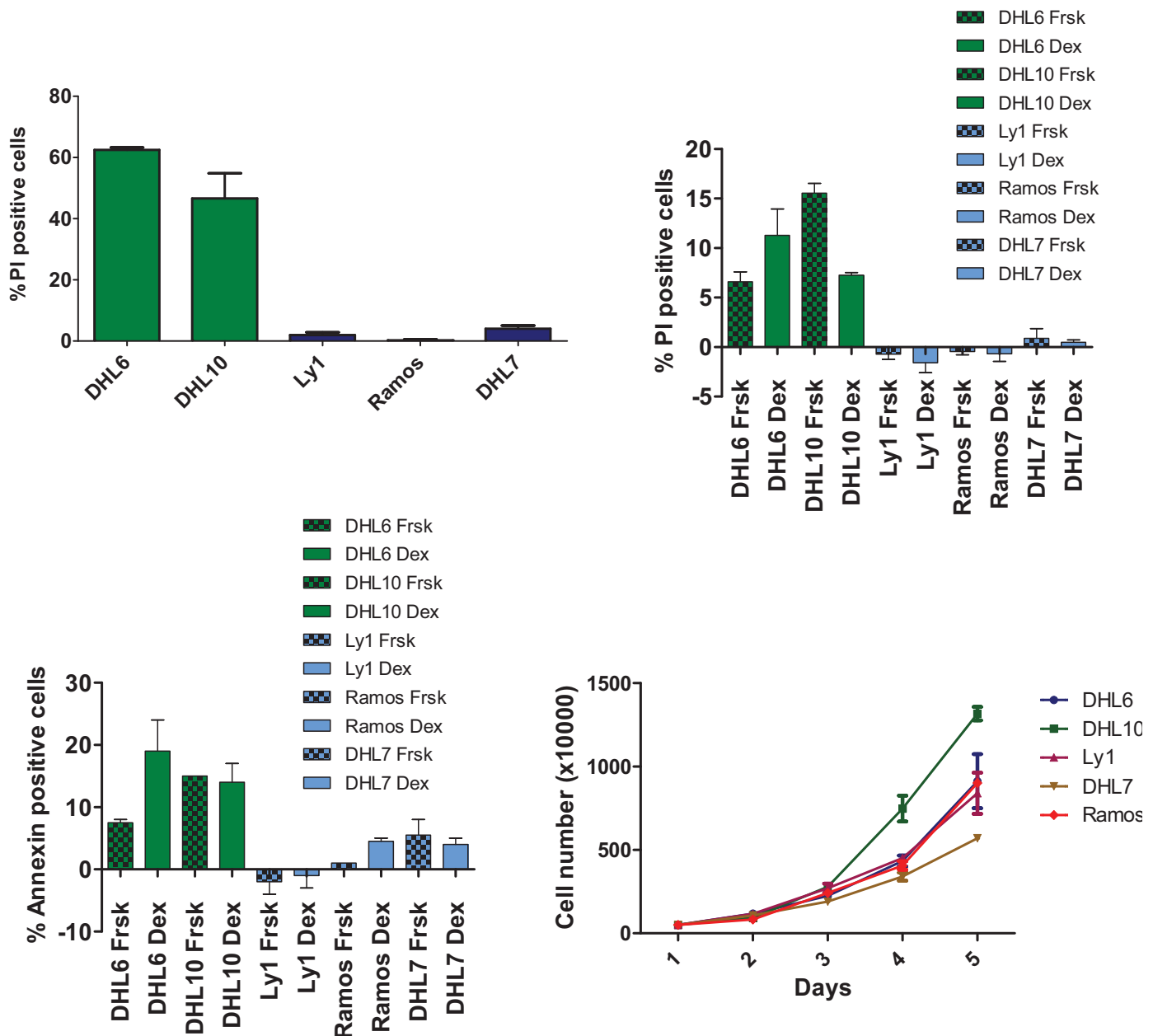


Figure S1B. Glucocorticoid-induced apoptosis in DLBCL cell lines. **Top left panel:** Propidium iodide staining demonstrate that in the presence of cAMP (forskolin, 5 μ M), DLBCL cell lymphoma cell lines expressing low-levels of PDE4B (DHL6 and DHL10) were markedly more sensitive to dexamethasone (100nM) than those B cell lymphomas expressing high PDE4B levels (Ly1, Ramos, DHL7) ($p < 0.05$ one-way ANOVA test). Data shown were collected 48h after drug exposure, represent the mean \pm SD of three independent experiments and were normalized by apoptosis rate of cells exposed exclusively to dexamethasone. **Top right panel:** Propidium iodide positive cells, the same data as in the left panel, but displayed as dexamethasone and forskolin treatments normalized by vehicle-treated cells. **Bottom left panel:** Annexin V positive cells, the same data as shown in Figure 1B in the manuscript, but displayed as dexamethasone and forskolin treatments normalized by vehicle-treated cells. **Bottom right panel:** A growth curve of these five DLBCL cell lines was constructed by manually counting the cells grown in RPMI 10% media (trypan blue exclusion method). These data show that the observed rate of apoptosis did not reflect a unique growth kinetic of these cells. Results shown are mean and SD of data generated in triplicate, and are representative of three independent experiments.

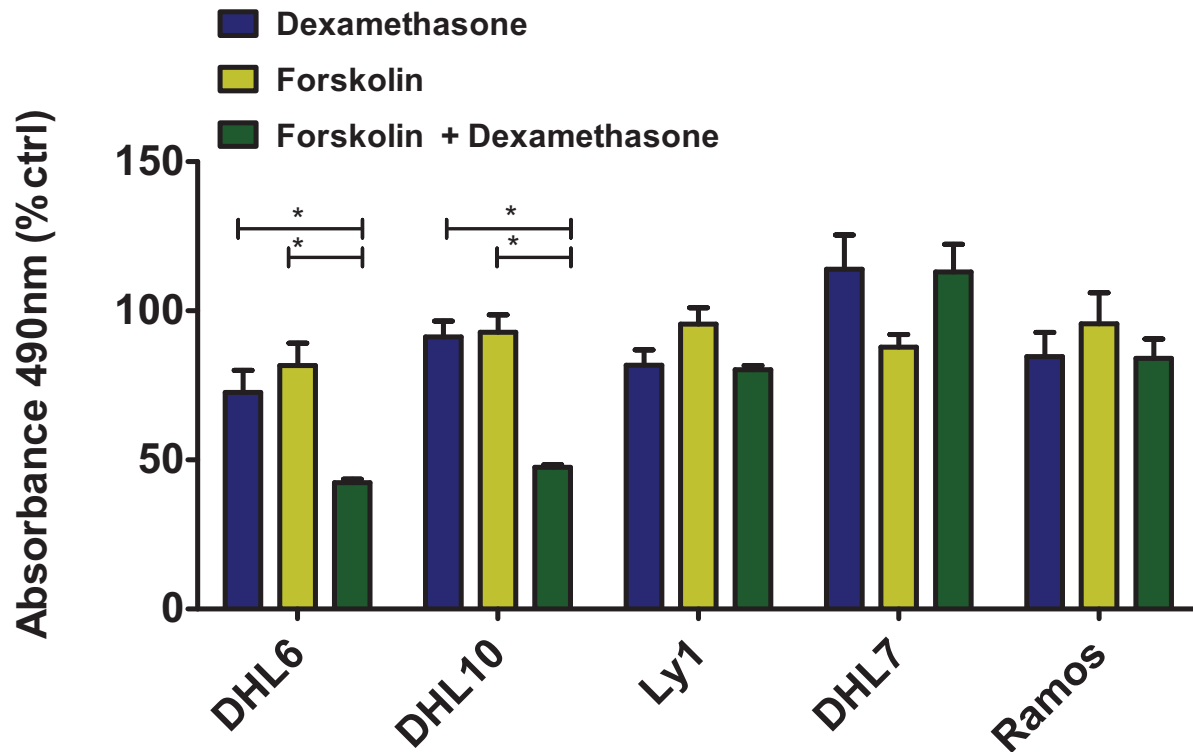


Figure S1C: Glucocorticoid activity in DLBCL expressing high or low PDE4B levels. Cell proliferation assays show that in the PDE4B-low (DHL6 and DHL10), but not in PDE4B-high (Ly1, DHL7, Ramos) B cell lymphoma cell lines dexamethasone (20nM) activity is significantly improved in the presence of cAMP (forskolin 5 μ M) (*, $p < 0.05$, one way ANOVA test, combination *versus* either agent alone). Importantly, at the concentrations used herein, forskolin did not induce any significant growth inhibition indicating that in this context, cAMP acted primarily as sensitizer of glucocorticoid activities, in a PDE4B-dependent manner. For these assays, cells were grown in 10%FBS media and proliferation results collected at 48h. The data shown represent mean and +/- SD of all data points from two independent experiments performed in duplicated; all assays were repeated no less than three times.

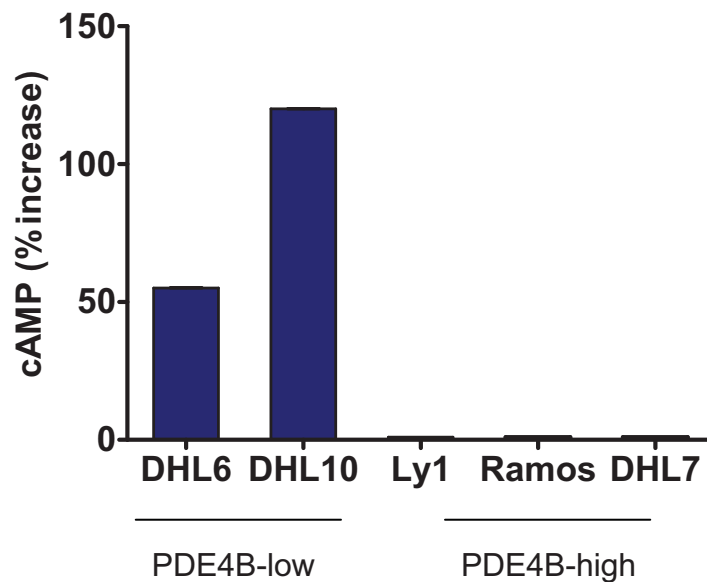
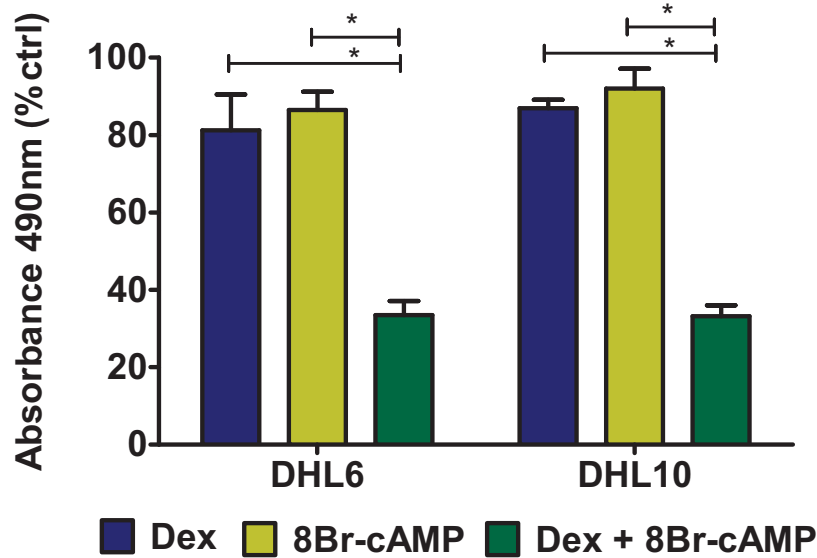


Figure S1D: Synthetic cAMP recapitulates the effects of forskolin and improves glucocorticoid activity in DLBCL expressing low levels of PDE4B. **Top.** Cell proliferation assays in the presence of 8-bromo-cAMP (2mM) show that this agent significantly enhances the growth inhibitory effects of dexamethasone (20nM) in PDE4B-low DLBCL cell lines (*, $p < 0.05$, one way ANOVA test, combination *versus* either agent alone). These data confirm that the forskolin effects on restoring glucocorticoid sensitivity derive from elevation of intracellular cAMP levels. In these assays, cells were grown in 2% FBS media and proliferation results collected at 48h. The data shown represent mean and +/- SD of all data points from two independent experiments performed in duplicate. **Bottom.** Quantification of intracellular cAMP following exposure to 8-bromo-cAMP confirms the relationship between PDE4B expression and the levels of this second-messenger in DLBCL cell lines.

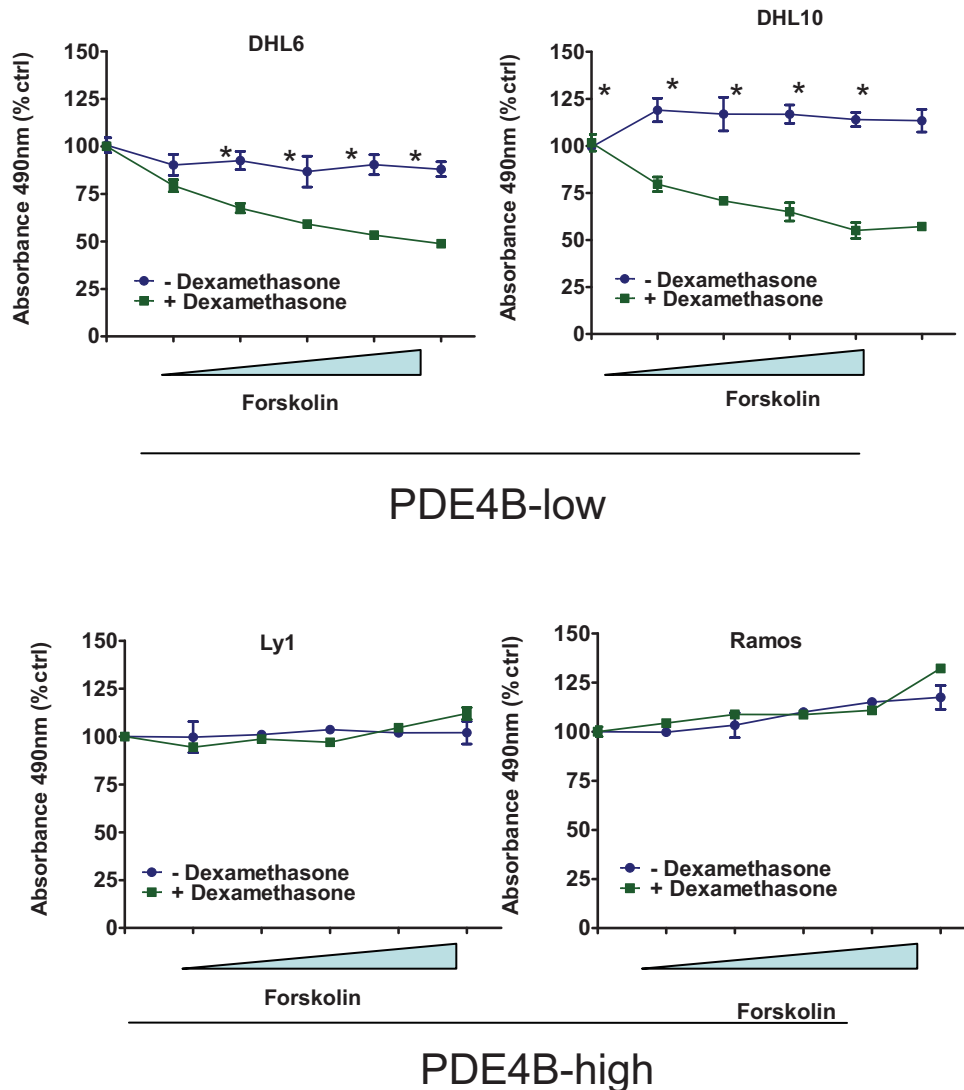


Figure S1E: Restoration of glucocorticoid sensitivity in B cell lymphomas is cAMP level-dependent. Cell proliferation assay in four independent B cell lymphoma cell lines highlight the “dose-dependent” effects of cAMP intracellular levels in significantly improving glucocorticoid activity (*, $p < 0.05$, two-tailed Student’s t-test), and confirm the central role of PDE4B in regulating these effects. In these assays, cells were grown in 10% FBS media, forskolin used from 1-5 μ M and dexamethasone at 50nM; proliferation results collected at 48h. The data shown represent mean and +/- SD of all data points from two independent experiments performed in duplicate.

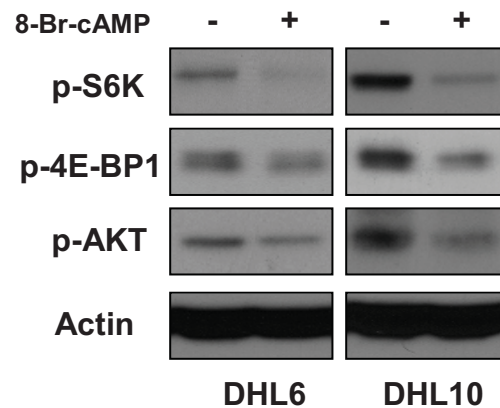


Figure S1F: Synthetic cAMP inhibits the AKT/mTOR pathway in PDE4B low DLBCL cell lines. Western blot analyses of the phosphorylation levels of AKT (S473), S6K (T389), 4E-BP1 (T37/46) in two independent PDE4B-low DLBCL following incubation with 8-Bromo-cAMP (2mM, DHL6 overnight; DHL10 for 48h) or vehicle control (-). The marked downregulation observed confirms the role of cAMP in regulating the activity of the AKT/mTOR pathway in DLBCL.

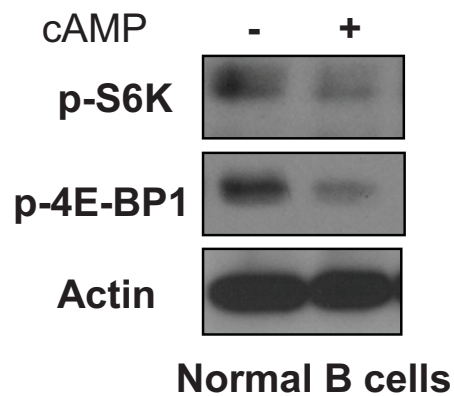


Figure S1G: cAMP inhibits mTOR activity in normal mature B-cells. Western blot analyses of S6K (T389) and 4E-BP1 (T37/46) phosphorylation levels in murine mature B-cells exposed to rabbit anti-mouse IgM (10 μ g/ml, 5 minutes) followed by forskolin (40 μ M, 1h) or vehicle control (-). cAMP-mediated downregulation of mTOR signals is readily detectable in these cells, highlighting the relevance of PDE4B's abnormally high expression and consequent blockade of this inhibitory axis in the pathogenesis of aggressive lymphomas. BCR cross-linking was used to allow measurement of phosphorylation in the investigated proteins; phospho-AKT levels remained below detection levels precluding the determination of cAMP effects under these conditions.

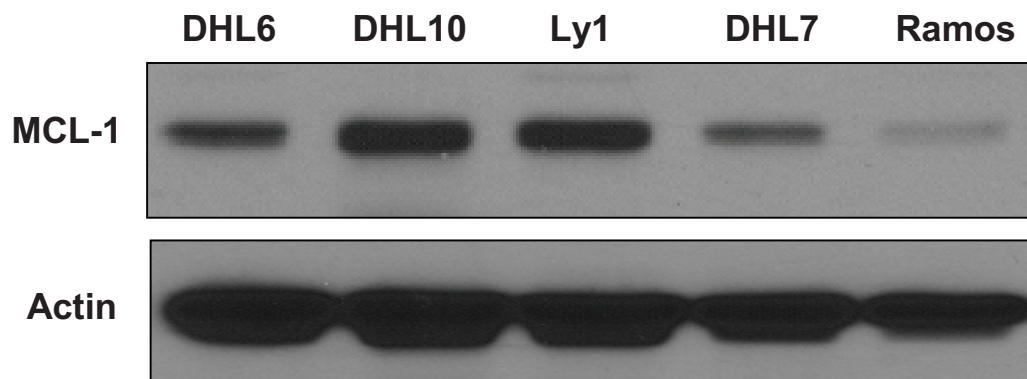


Figure S1H: Baseline MCL1 expression does not predict glucocorticoid sensitivity in B cell lymphomas. Western blot analyses of MCL1 expression in five independent B cell lymphoma cell lines indicate a lack of predictive value in determining response to dexamethasone. In brief, whereas the expression of MCL1 varied significantly amongst these cells, all were resistant to dexamethasone used as a single agent (see supplementary figures 1C and 1E above).

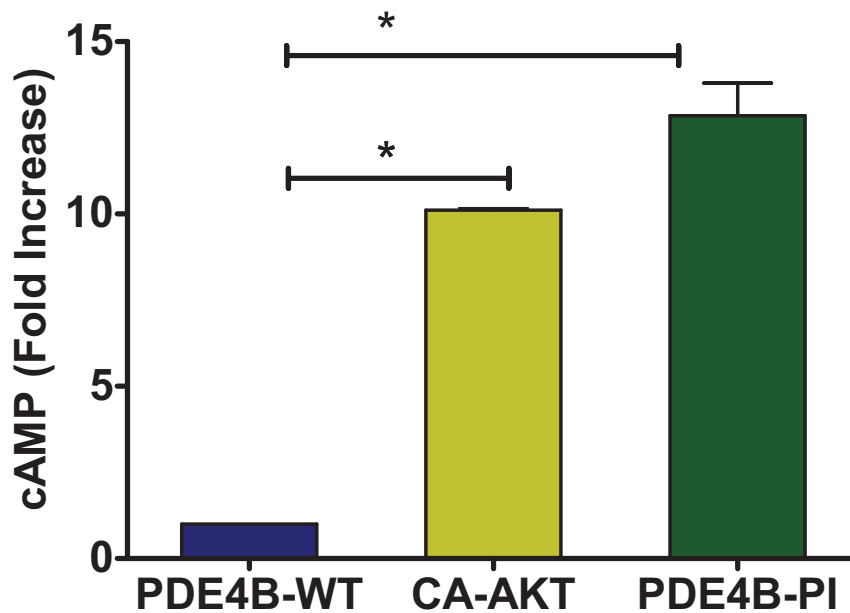


Figure S2A: Cyclic-AMP levels in DLBCL cell lines stably expressing PDE4B-WT, PDE4B-PI or CA-AKT. The relevant DHL6 cells were grown in RPMI 10% media, incubated with forskolin (40 μ M) for 15 minutes and intracellular cAMP measured thereafter. Marked elevation (*, $p < 0.05$, one way ANOVA test) in the levels of this second messenger was noted in PDE4B-PI and CA-AKT cells but not in the presence of a functional PDE4B gene. The data shown represent mean and +/- SD of all data points from two independent experiments performed in duplicate.

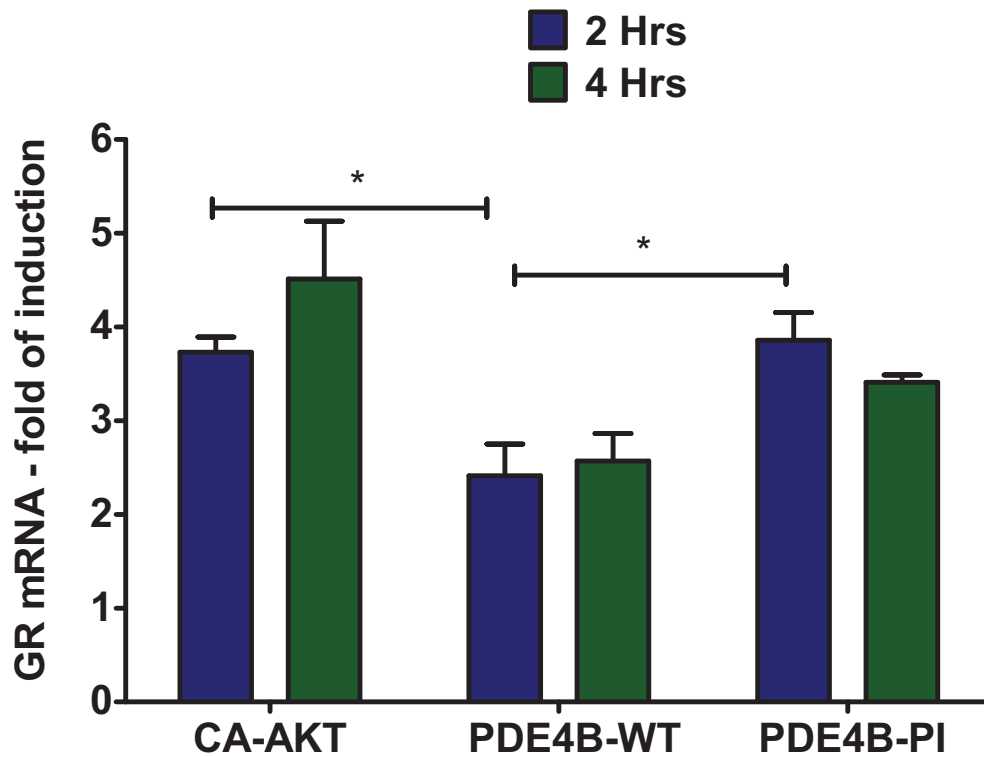


Figure S2B: cAMP-mediated induction of glucocorticoid receptor (GR) expression in DLBCL cell lines stably expressing PDE4B-WT, PDE4B-PI or CA-AKT. Real-time RT-PCR measurements show that induction of GR expression is lower in PDE4B-WT cells than in PDE4B-PI or CA-AKT cells (*, $p < 0.05$, one way ANOVA test); no statistically significant difference was found between CA-AKT and PDE4B-PI, despite the fact that the former is resistant to GC effects (Figure 2B). In the relevant cell lines, grown in RPMI 10% media, incubated with forskolin ($10\mu\text{M}$) for 2 and 4 hours. Data shown is mean \pm SD of all data points from two independent experiments performed in duplicate, and reflect the fold of induction of the GR (including isoforms alpha and beta) relative to the vehicle treated cells.

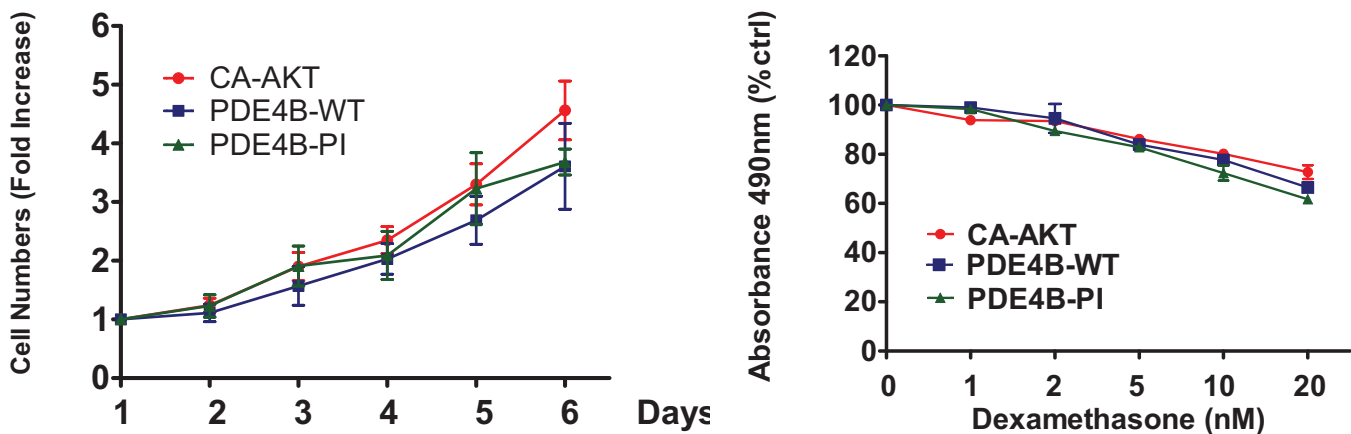


Figure S2C. Proliferation of DLBCL cell lines stably expressing PDE4B-WT, PDE4B-PI or CA-AKT. Growth rate of the relevant cell lines at baseline (left panel) or following dexamethasone exposure (right panel) was determined by cell count and with MTS assay, respectively. These similar growth patterns observed indicate that the effects of AKT and PDE4B overexpression on glucocorticoid sensitivity (Figure 2B) are related to their activity towards cAMP. For the dexamethasone treatment (0-20nM), cells grown in RPMI 10% and data collected at 72h. Curves shown are the mean \pm SD of a representative experiment performed in duplicate and repeated twice. The growth curve of these three independent populations was constructed by manually counting the cells grown in RPMI 10% media (trypan blue exclusion method). Data show are mean \pm SD of two independent experiments performed in triplicate.

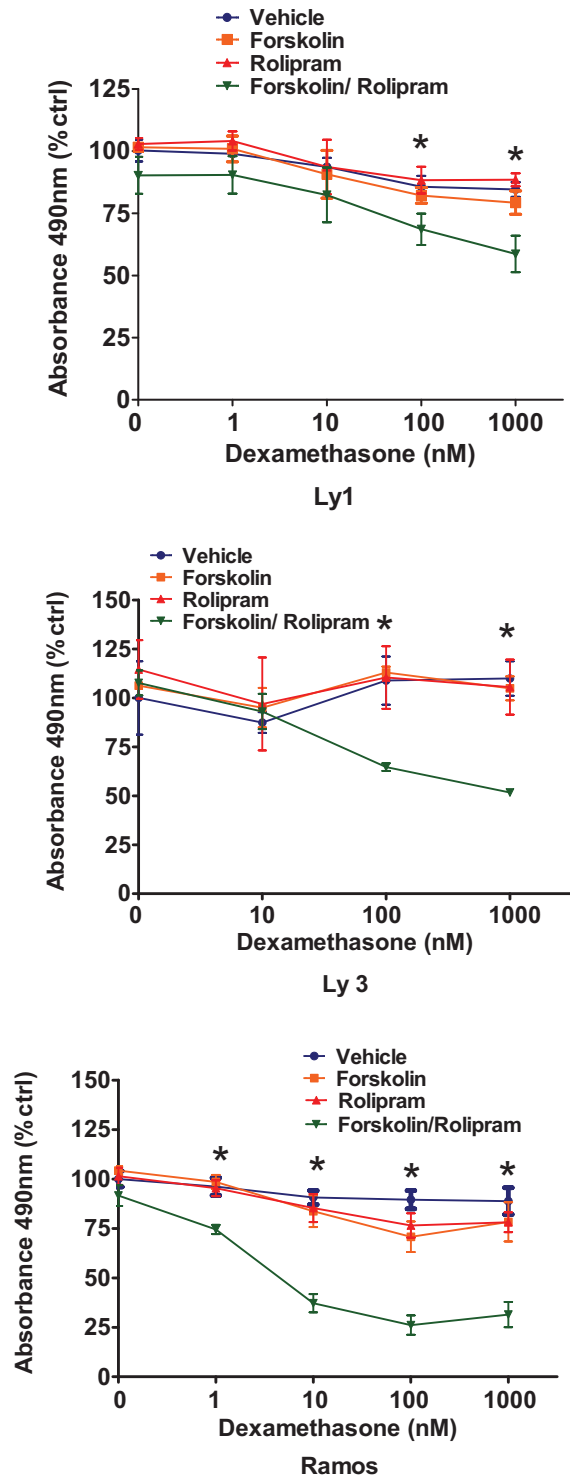


Figure S3A. PDE4 inhibition with rolipram significantly improves glucocorticoid activity in B cell lymphoma. In three independent B cell lymphoma cell lines that express high levels of PDE4B, treatment with the PDE4-specific inhibitor rolipram in presence of cAMP (forskolin) resulted significantly higher, dose-dependent, activity of dexamethasone (1-1000nM) (*, $p < 0.05$, one way ANOVA test). In agreement with the high expression of PDE4B and low basal activity of adenylyl cyclases in these cells, forskolin (20-40 μ M) or rolipram alone (10-20 μ M) had limited effect on cell proliferation. Data shown are mean and SD of all data points from experiments performed in duplicate and collected at 72h (Ly1 and Ramos) or in triplicate and collected at 96h (Ly3), normalized by vehicle treated cells (no dexamethasone).

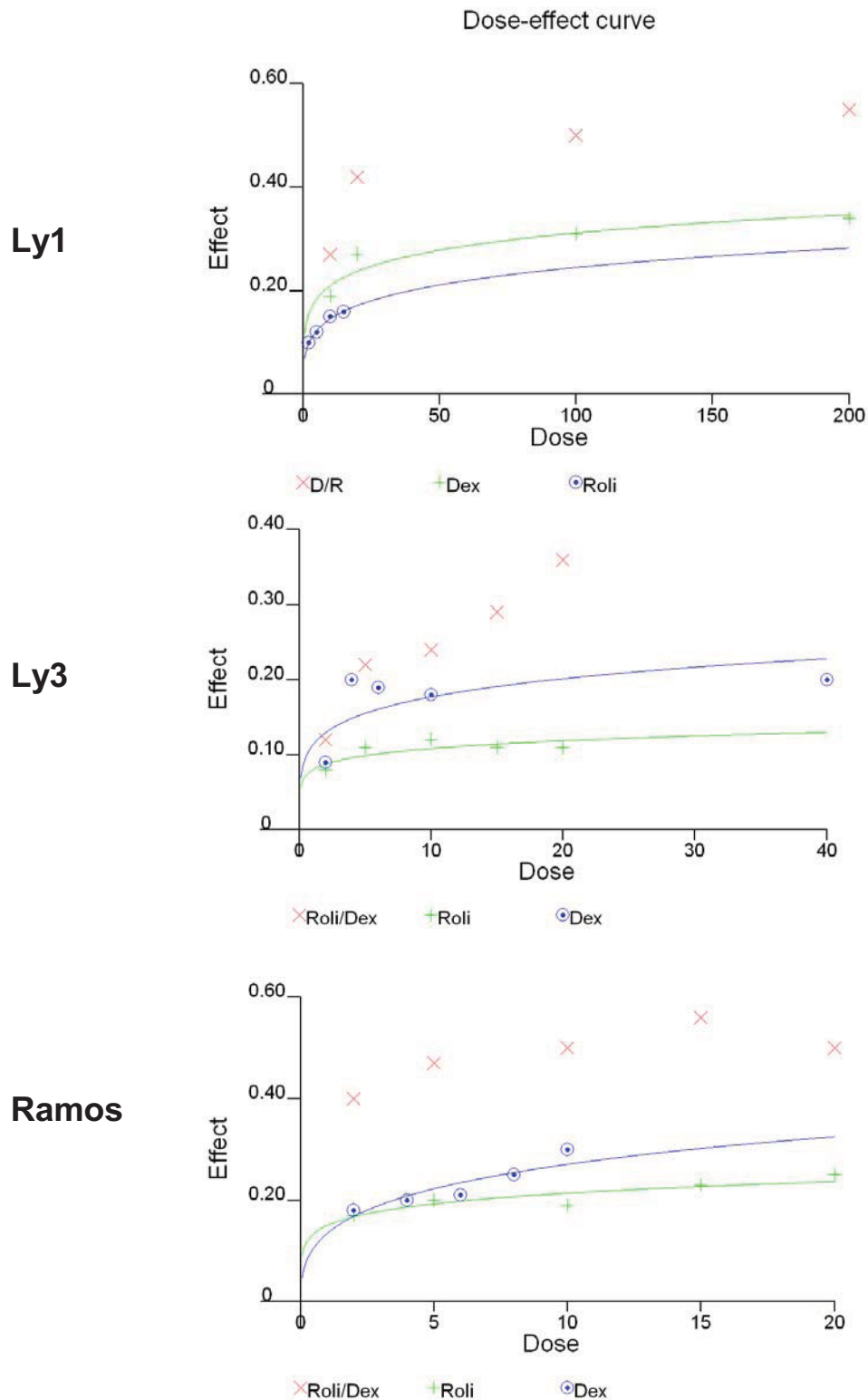


Figure S3B. Synergistic combination of rolipram and dexamethasone in B cell lymphoma. Dose-effect curves were calculated with the CalcuSyn software (Biosoft, Cambridge, UK) and used to generate the combination index (CI, Table 1), which demonstrates that these drugs are highly synergistic in the cell lines studied. For these MTS-based proliferation assays, cells were grown in RPMI 10% and data collected at 72h. For the Ly1 cell line the dexamethasone dose varied from 10-200nM, for Ly3 from 2-40nM and for Ramos from 2-10nM. Rolipram was used from 2-20 μ M in all three cell lines. The experiments were performed in duplicate and repeated twice. Dex= Dexamethasone, Roli= Rolipram, R/D= Rolipram + Dexamethasone.

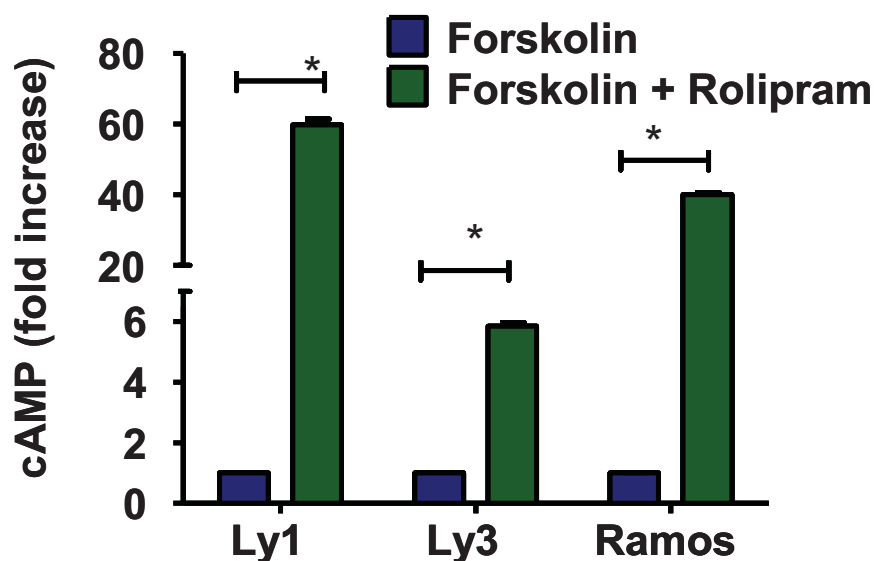


Figure S3C. PDE4 inhibition with rolipram significantly increase the intracellular levels of cAMP. In all three aggressive lymphoma models studied, inhibition of PDE4 with rolipram (20 μ M for 1h, Ly1 and Ly3, or 72 hours, Ramos) in the presence of forskolin (10 μ M, Ly1 and Ly3 for 1hour, or 20 μ M Ramos for 72 hours) resulted in marked elevation of cAMP levels (*, $p < 0.05$, two-sided Student's t-test). Data shown are mean \pm SD and normalized by cells exposed exclusively to forskolin.

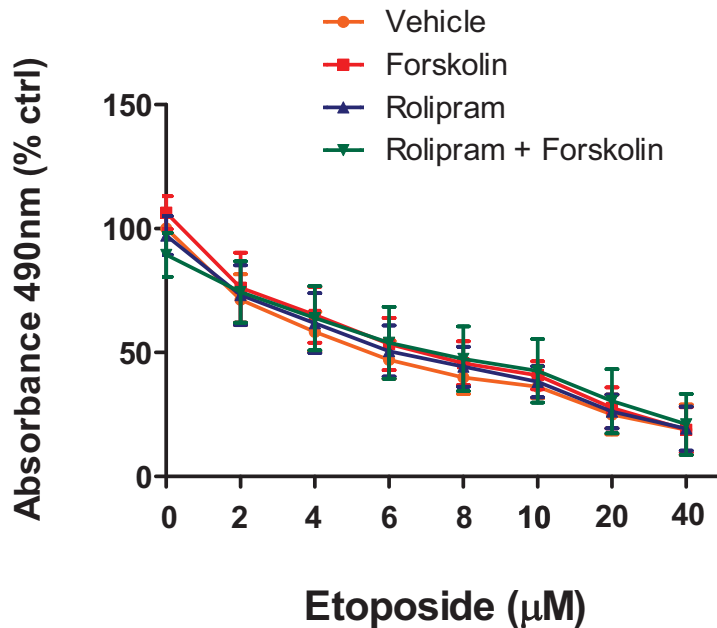
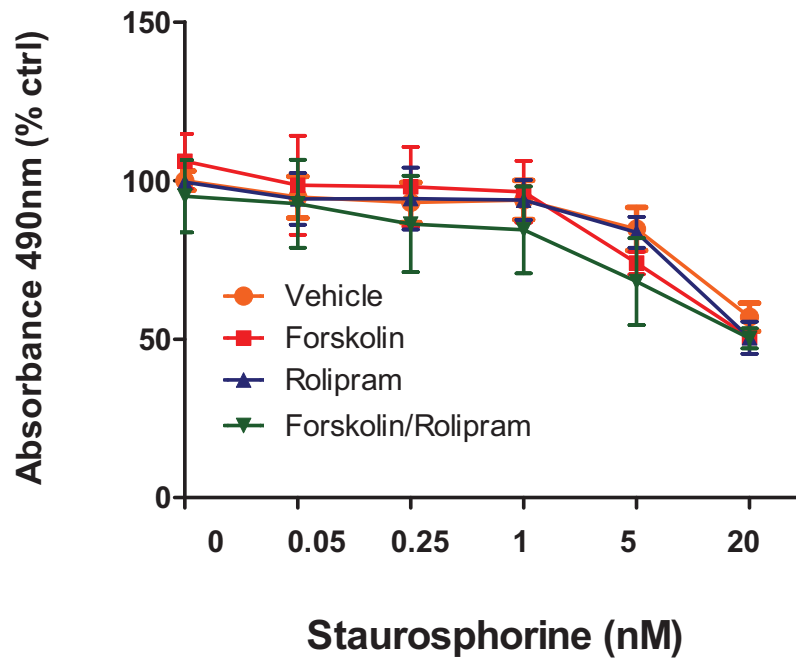


Figure S3D. PDE4 inhibition does not impact on the effectiveness of broad chemotherapeutic agents in B cell lymphoma. Cell proliferation assays were performed in the PDE4B high Ramos cell line grown in RPMI 10% with increasing doses of etoposide (2 - 40µM) or staurosporine (.05-20nM) in the presence of vehicle, forskolin (20µM), rolipram (20µM) or both drugs combined. Modulation of PDE4 activity and cAMP levels with these compounds did not modify the activity of the tested chemotherapeutic agents. Data shown were collected at 72 hours, normalized by vehicle treated cells, represent the mean +/- SD from all data points from two independent replicates.

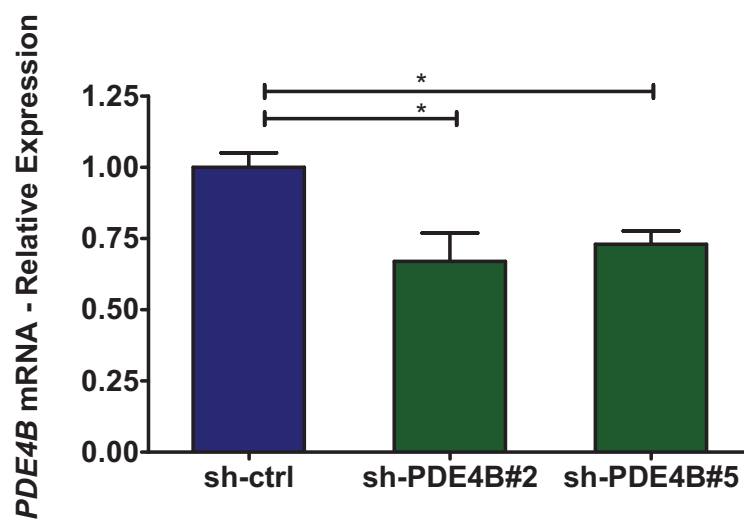


Figure S3E. PDE4B levels in B cell lymphoma cell lines stably expressing PDE4B shRNA constructs. Real-time RT-PCR measurements confirm the downregulation of *PDE4B* in Ramos cell line clones ectopically expressing two independent constructs (shRNA#2 and shRNA#5) directed at *PDE4B* (*, $p < 0.05$, one way ANOVA test). The assays were performed in triplicate and the *PDE4B* expression was corrected by the expression of the TATA-binding protein (TBP) gene. Data are displayed as relative expression normalized to the *PDE4B* expression in shRNA control cells and determined using the $\Delta\Delta CT$ method and reported as $2^{-\Delta\Delta CT}$

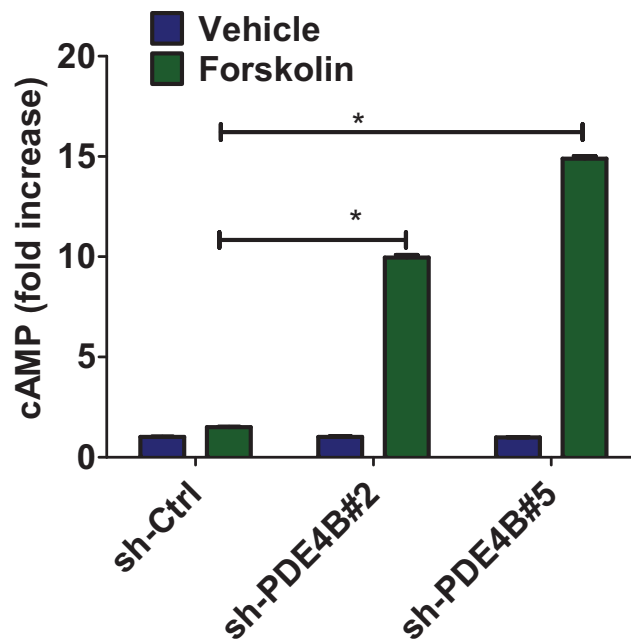


Figure S3F. ShRNA-based PDE4B knock-down significantly increases the intracellular levels of cAMP. Ramos cell line clones ectopically expressing two independent constructs (shRNA#2 and shRNA#5) directed at PDE4B have a significantly higher cAMP levels than their siogenic controls expressing a shRNA-control construct (*, $p < 0.05$, one way ANOVA test). Cells were grown in RPMI 10%, exposed to vehicle or forskolin (40 μ M) for 48 hours. Data shown are mean \pm SD of an experiment performed in triplicate.

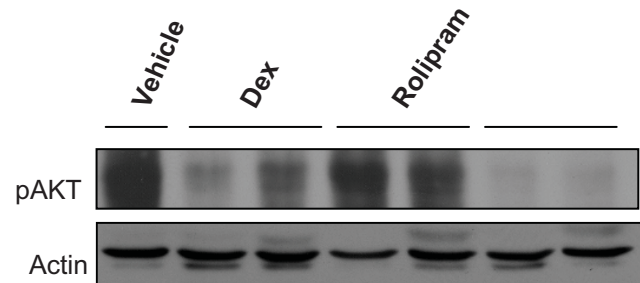
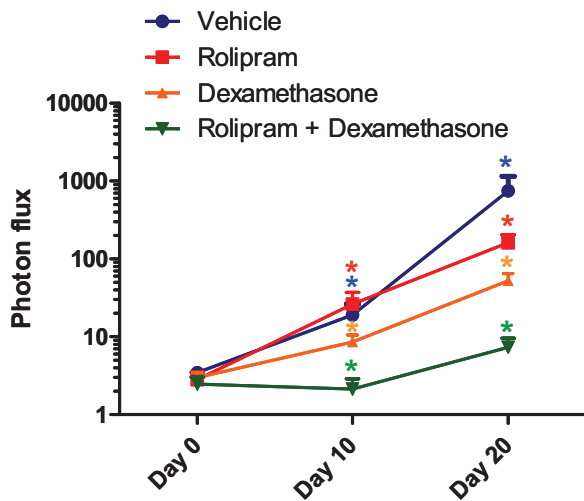
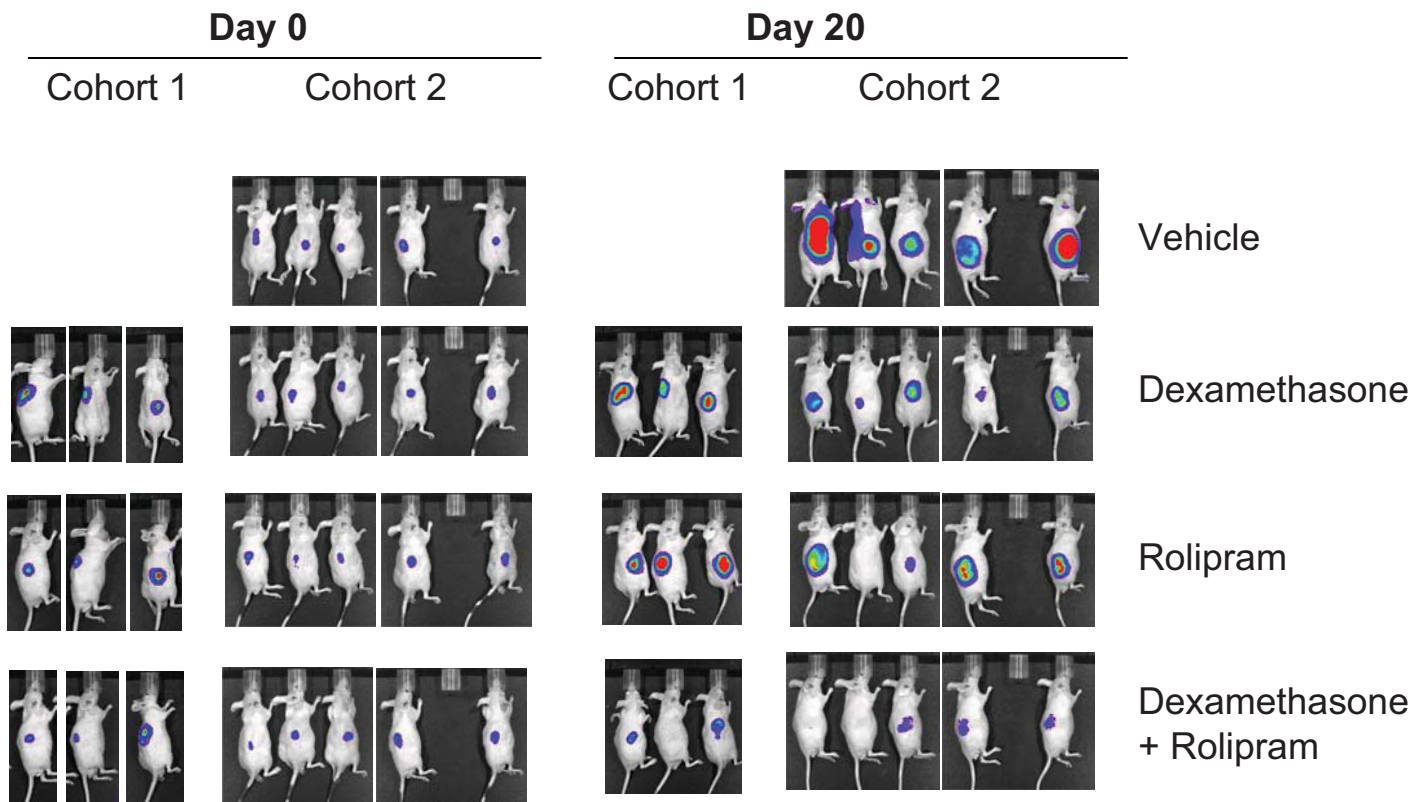


Figure S3G. Anti-lymphoma activity of PDE4 inhibitors and/or glucocorticoids in vivo. Bioluminescent imaging of mice inoculated with Ramos cells stably expressing the luciferase gene. Images shown are from two independent cohorts (n=29) at day 0 (72 hours post cell inoculation) or at the 20th day of treatment with vehicle (1%DMSO in water, IP daily) dexamethasone (15mg/kg, IP daily), rolipram (10mg/kg, IP daily) or the combination or both agents. The photon flux-based quantification of tumor size and spread is shown in Figure 3E, and confirms the statistically significant improvement in glucocorticoid activity following its rational combination with a PDE4 inhibitor (*, $p < 0.05$, Kruskal-Wallis Test). V= Vehicle. Protein was isolated from an independent group of xenografts (not shown), and western blotting used to characterize the differential downmodulation of phospho-AKT in the various treatment arms (right panel).